High-throughput in vivo screening of targeted molecular imaging agents

M. Karen J. Gagnon[a], Sven H. Hausner[a], Jan Marik[a], Craig K. Abbey[a,b], John F. Marshall[c], and Julie L. Sutcliffe[a,d,1]

[a]Department of Biomedical Engineering, [d]Center for Molecular and Genomic Imaging, University of California, Davis, CA 95616; [b]Department of Psychology, University of California, Santa Barbara, CA 93106; and [c]Center for Tumor Biology, Barts and London Medical School, London EC1M 6BQ, United Kingdom

Communicated by Michael E. Phelps, University of California, Los Angeles, CA, August 17, 2009 (received for review October 15, 2008)

The rapid development and translation of targeted molecular imaging agents from bench to bedside is currently a slow process, with a clear bottleneck between the discovery of new compounds and the development of an appropriate molecular imaging agent. The ability to identify promising new molecular imaging agents, as well as failures, much earlier in the development process using high-throughput screening techniques could save significant time and money. This work combines the advantages of combinatorial chemistry, site-specific solid-phase radiolabeling, and in vivo imaging for the rapid screening of molecular imaging agents. A one-bead-one-compound library was prepared and evaluated in vitro, leading to the identification of 42 promising lead peptides. Over 11 consecutive days, these peptides, along with a control peptide, were successfully radiolabeled with 4-[^{18}F]fluorobenzoic acid and evaluated in vivo using microPET. Four peptides were radiolabeled per day, followed by simultaneous injection of each individual peptide into 2 animals. As a result, 4 promising new molecular imaging agents were identified that otherwise would not have been selected based solely on in vitro data. This study is the first example of the practical application of a high-throughput screening approach using microPET imaging of [^{18}F]-labeled peptides for the rapid in vivo identification of potential new molecular imaging agents.

high-throughput screening | in vivo imaging | microPET | radiolabeled peptides | positron emission tomography

Combinatorial chemistry (1, 2) and phage display (3) techniques have become essential tools for the production of large compound libraries, which can be rapidly produced for the discovery of new drugs. Designing and implementing high-throughput screening (HTS) approaches to identify lead compounds that show affinity for a biological target from these large libraries, wherein millions of new compounds may exist, is often accomplished through in vitro screening. In general, the 2 approaches by which this can be accomplished are either solution-phase screening techniques (4–11), generally used by drug discovery programs, or solid-phase screening, which has garnered interest for the evaluation of libraries prepared using combinatorial chemistry.

Though there are many reports outlining high-throughput approaches for in vitro screening, few exist where the sole purpose is to develop high-throughput in vivo methodologies for the identification of new molecular imaging agents. While the feasibility of using magnetic resonance imaging (MRI) for high-throughput applications has been explored with both the development of scanner technology and the scanning of multiple animals in parallel (12–20), positron emission tomography (PET) has received very little attention for high-throughput applications. This is likely the result of the unique set of problems that arise when considering using the latter imaging modality. The half-lives of the radioactive isotopes commonly used for PET are short, typically only minutes, meaning that incorporation of the radioactive isotope into the compound of interest, as well as the subsequent in vivo imaging, must occur rapidly to obtain satisfactory results. In addition, the chemistry required to furnish the desired radiolabeled compound must be robust and provide the compound with a high specific activity. Though these requirements have limited the use of PET for in vivo HTS, the feasibility of using PET, in combination with computed tomography (CT), has been briefly explored as a potential method for this purpose (21). As described by Hofmann et al. (21), a clinical high-resolution PET/CT scanner was fitted with an 18-slot small-animal holding device, and 10 anesthetized animals that had been administered a single gallium-68 labeled peptide (^{68}Ga-DOTATOC) were placed inside and PET/CT images acquired. After 20 min using PET/CT fusion mode, significant delineation of the organs was observed, leading to the conclusion that if all 18 slots were used at once, 18 animals could be scanned in ~20 min. Presumably, if each animal in the holding device was injected with a different radiolabeled compound, 18 different compounds could be evaluated in a high-throughput manner. In summary, much of the focus on developing high-throughput in vivo screening techniques has rested on advancing scanner and/or animal handling technology, whereas very little has focused on the development of high-throughput methodologies for the screening of large numbers of potential new molecular imaging agents.

Our approach to identify potential new molecular imaging agents in a high-throughput manner takes advantage of the one-bead-one-compound (OBOC) library approach (a high-throughput method for the production of peptide libraries), fast and efficient solid-phase radiolabeling, and in vivo imaging using PET. The OBOC approach (1, 2) has been successfully used for the identification of new ligands for unique cell-surface receptors of prostate, ovarian, and lung cancer, as well as T- and B-cell lymphoma (22). In addition, highly focused libraries have been prepared using the OBOC approach, resulting in the identification of a new peptidomimetic for imaging $\alpha_4\beta_1$-expressing lymphomas in vivo (23). The OBOC approach uses combinatorial chemistry to produce a library of compounds, most commonly peptides, on an insoluble bead. Though only one compound or peptide sequence is present on each individual bead, there are over 10^{13} copies of that particular compound on each bead (24). Using this approach, millions of unique compounds can be produced in a high-throughput fashion. In many cases, several lead compounds are identified following stringent in vitro testing, but, in general, only the most promising single compound based on in vitro screening is selected for further in vivo evaluation. While in vitro screening may identify promising lead compounds, it is widely accepted that in vitro success does not always correspond to in vivo success; as a result, many compounds with favorable in vivo characteristics may be overlooked. An in vivo method to rapidly screen new compounds for specific biological targeting is therefore useful in terms of deciding which compounds may be candidates for further development, allowing not only promising compounds, but also failures, to be identified much earlier in the development process (i.e., providing a go or no-go decision to be made sooner).

Author contributions: M.K.J.G., S.H.H., J.M., and J.L.S. designed research; M.K.J.G., S.H.H., and J.M. performed research; J.F.M. contributed new reagents/analytic tools; M.K.J.G., C.K.A., and J.L.S. analyzed data; and M.K.J.G. and J.L.S. wrote the paper.

The authors declare no conflict of interest.

[1]To whom correspondence should be addressed. E-mail: jlsutcliffe@ucdavis.edu.

This article contains supporting information online at www.pnas.org/cgi/content/full/0906925106/DCSupplemental.

In an effort to increase the number of compounds that can be screened in vivo, we have developed a unique approach wherein 42 compounds identified from in vitro screening assays were labeled with the radioactive isotope fluorine-18 ($t_{½}$ = 110 min) using solid-phase radiolabeling techniques and evaluated in vivo using microPET. Solid-phase radiolabeling has been shown to be an efficient and reliable method for the incorporation of the fluorine-18-bearing prosthetic group 4-[^{18}F]fluorobenzoic acid ([^{18}F]FBA) into resin-bound peptides yielding the desired radiolabeled peptide in quantities sufficient for in vivo imaging (25, 26). Although the $\alpha_v\beta_6$ integrin was chosen as the model target for this HTS study, this approach can be applied to the identification of molecular imaging agents that target any cell surface receptor. The $\alpha_v\beta_6$ integrin is an interesting target because although its expression is generally low or undetectable in normal epithelium, upregulation of this integrin has been linked with multiple types of cancer and was recently identified as a prognostic indicator for such diseases (26–30). Herein we report the combination of OBOC chemistry and solid-phase radiolabeling for the implementation of a high-throughput in vivo methodology for the identification of previously uncharacterized fluorine-18 radiolabeled molecular imaging agents for the $\alpha_v\beta_6$ integrin.

Results

In Vitro Lead Peptide Identification. The OBOC technique was used to prepare several peptide libraries based on the peptide sequence X^1X^2DLX^5X^6LX^8 (DLXXL is a motif that has been shown to enhance binding of peptides to the $\alpha_v\beta_6$ integrin) (31). The libraries were screened in vitro using a stringent double-positive cell-growth-on-bead assay (32) wherein the peptidic beads were incubated with cells expressing the $\alpha_v\beta_6$ integrin. To ensure the stringency of the assay, beads that were 90% covered in cells after incubation with the $\alpha_v\beta_6$-expressing cells in the positive screens or completely void in the negative screens were chosen. Sequences were identified using Edman degradation. In preparation of further in vitro analysis, the identified sequences were resynthesized on the acid labile Rink amide resin using standard fluorenylmethoxycarbonyl (Fmoc) chemistry. A total of 55 sequences were N-terminally modified with 4-[^{19}F]fluorobenzoic acid (FBA) and evaluated using ELISA against immobilized recombinant $\alpha_v\beta_6$, the integrin of interest, as well as $\alpha_v\beta_3$, $\alpha_v\beta_5$, $\alpha_5\beta_1$, and $\alpha_{IIb}\beta_3$. Based on the ELISA results, the FBA-modified sequences were ranked according to their binding selectivity and/or affinity for the $\alpha_v\beta_6$ integrin.

We have assigned good selectivity as FBA-modified peptides that bind to the target $\alpha_v\beta_6$ integrin and have minimal binding (i.e., >100 μM) to the other related integrins evaluated ($\alpha_v\beta_3$, $\alpha_v\beta_5$, $\alpha_5\beta_1$, and $\alpha_{IIb}\beta_3$). For example, one FBA-modified peptide identified from this study had an IC_{50} for the $\alpha_v\beta_6$ integrin of 36 nM; however, this peptide had no binding to the other 4 integrins evaluated, making this peptide selective for the $\alpha_v\beta_6$ integrin. All peptides classified as selective for the $\alpha_v\beta_6$ integrin had a minimum of a 2-fold difference in binding to the $\alpha_v\beta_6$ integrin over the $\alpha_v\beta_3$ integrin (maximum: 18,000-fold difference; average difference ≈3,100-fold) and no binding or binding at a peptide concentration >100 uM to the other 3 integrins evaluated.

Correspondingly, we have assigned good affinity as FBA-modified peptides which, although they may have had some degree of binding to one or all of the other integrins, had significant binding to the $\alpha_v\beta_6$ integrin. For example, a second FBA-modified peptide also identified from this study had an IC_{50} of 5 nM for the $\alpha_v\beta_6$ integrin, as well as some binding to the $\alpha_v\beta_3$ integrin (500 nM) and the $\alpha_{IIb}\beta_3$ integrin (1 μM). As a result, this peptide was classified as having a high affinity for the $\alpha_v\beta_6$ integrin. The peptides classified as having a high affinity for the $\alpha_v\beta_6$ integrin had IC_{50}s ranging from 5 nM to 15 μM.

Applying both the selectivity and affinity ranking criteria to all 55 of the prepared FBA-modified peptides, we identified 25 peptides that displayed good selectivity and 43 peptides that displayed good affinity for the $\alpha_v\beta_6$ integrin. Combining these 2 data sets and eliminating duplicates we identified 42 unique sequences with high affinity and/or selectivity. The complete list of peptides identified, as well as their binding to the 5 integrins evaluated, is available in the *SI Text*. The 4 best peptides in terms of selectivity and the 4 best peptides in terms of affinity are summarized in Table 1. The top 4 peptides with good selectivity for the target integrin (FBA-RDDLMYLR, FBA-RLDLQPLI, FBA-PMDLAYLR, and FBA-RVDLMYLR) had IC_{50}s ranging from 36 nM to 50 μM. Though the first 3 peptides displayed no binding to any of the 4 other integrins evaluated, FBA-RVDLMYLR displayed some binding to the $\alpha_{IIb}\beta_3$ integrin at concentrations greater than 100 μM. Although these peptides had somewhat mediocre IC_{50}s, they were of interest because of their selectivity for the $\alpha_v\beta_6$ integrin. The top 4 peptides with significant affinity for the $\alpha_v\beta_6$ integrin (FBA-RGDLIPLL, FBA-RGDLIALL, FBA-RGDLiPLL, and FBA-rGDLIPLL) were all derived from the parent sequence RGDLIPLL via alanine walks or substitution with D-amino acids. The sequence RGDLIPLL was the only RGD-containing sequence identified from the library and, because of its high affinity for the $\alpha_v\beta_6$ integrin, was subjected to further investigation, leading to the derivatives listed above. These top 4 high-affinity peptides all had IC_{50}s for the $\alpha_v\beta_6$ integrin of 5 nM; however, these peptides also displayed notable binding to both the $\alpha_v\beta_3$ and the $\alpha_{IIb}\beta_3$ integrins as expected because of the RGD motif.

Table 1. Top-ranked peptides identified from in vitro assays

Selectivity		Affinity	
Peptide sequence	IC_{50}	Peptide sequence	IC_{50}
FBA-RDDLMYLR	36	FBA-RGDLIPLL	5
FBA-RLDLQPLI	130	FBA-RGDLIALL	5
FBA-PMDLAYLR	50 μM	FBA-RGDLiPLL	5
FBA-RVDLMYLR	55	FBA-rGDLIPLL	5

The 4 top-ranked peptides in terms of selectivity and affinity are shown along with their respective IC_{50}s (expressed in nM, unless otherwise noted) for the $\alpha_v\beta_6$ integrin. IC_{50}s were determined in vitro using competitive binding assays. A total of 25 peptide sequences were identified as being highly selective for the $\alpha_v\beta_6$ integrin, and 43 peptides were identified as having a high affinity for the $\alpha_v\beta_6$ integrin. Comparing the 2 data sets and eliminating any peptides that appeared on both, we were able to identify 42 peptides that appeared to have favorable in vitro characteristics and were of interest for in vivo evaluation.

Radiolabeling and in Vivo Imaging. The 42 peptides identified from the libraries, as well as A20FMDV2 (which served as the "gold standard"), were radiolabeled with [^{18}F]FBA and evaluated in vivo using microPET over the span of 11 consecutive days. A20FMDV2 is a peptide comprised of 20 aa and was chosen as the gold standard because of its well-defined binding to the $\alpha_v\beta_6$ integrin in vivo in the same mouse model (26). A complete list of peptides evaluated, as well as their IC_{50}s, is listed in Table S1. Each day, 4 different peptides were N-terminally radiolabeled with [^{18}F]FBA in parallel using previously published solid-phase radiolabeling techniques (25) and purified using HPLC, yielding peptides with an average radiochemical purity of 98.1% ± 3.7%. Representative HPLC traces of several radiolabeled peptides are available in *SI Text* (Figs. S1–S6). The specific activity of the purified peptides, as determined by HPLC, was found to be >1 Ci/μmol. Each individual peptide was simultaneously injected via tail-vein catheter into 2 animals bearing paired tumors ($\alpha_v\beta_6$ positive and $\alpha_v\beta_6$ negative) (26), and microPET images were acquired. Scanning 4 pairs of mice a day at 5 timepoints yielded 40 scans per day (in 2 instances we were unable to obtain a final scan at 180 min; on one day only 3 pairs of mice were scanned). For the entirety of the 11-day study we obtained a total of 428 images. Throughout the study there were no failures, either

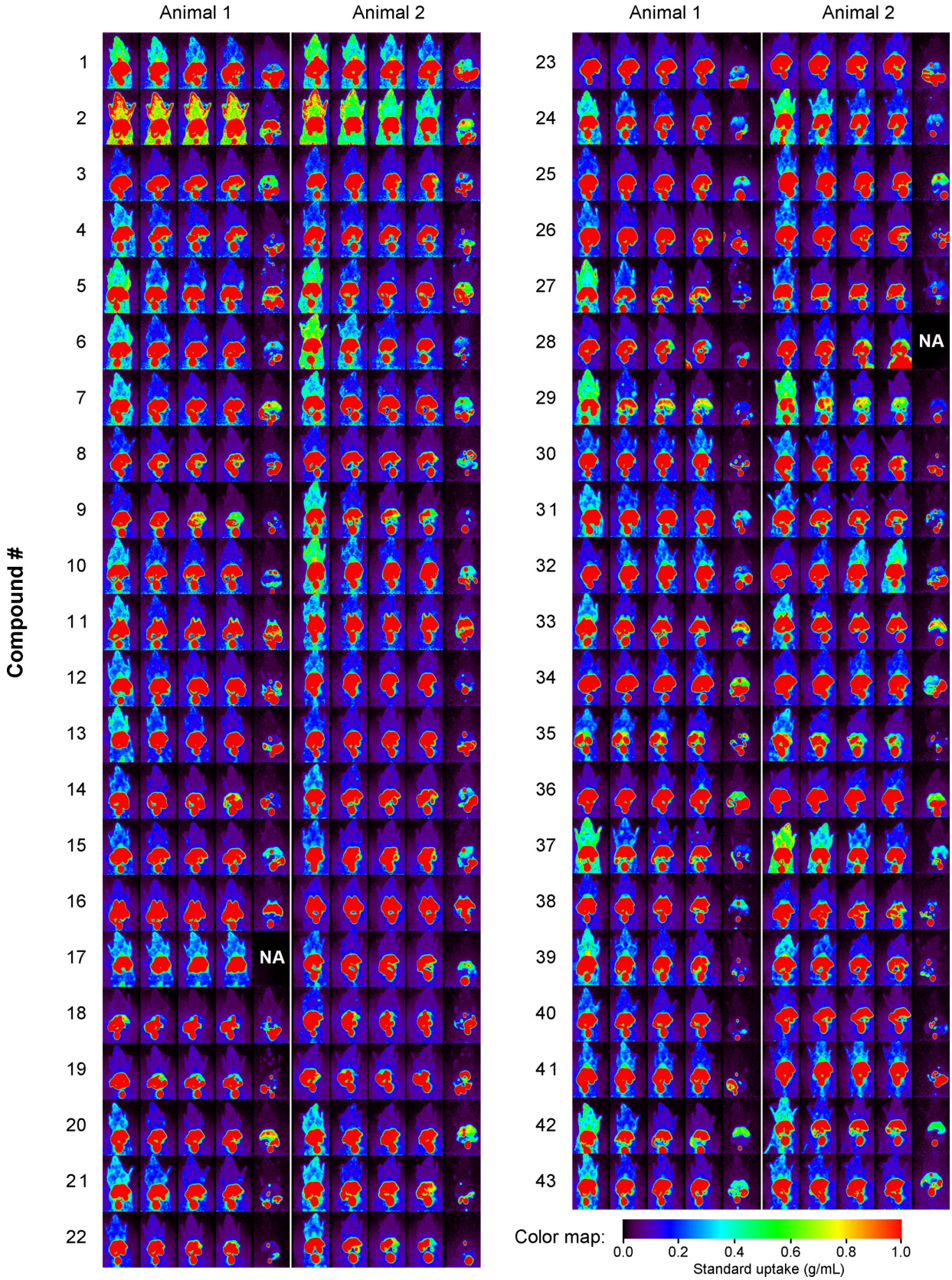

Fig. 1. MIP images of the 43 peptides evaluated in vivo using microPET. The 4 panels show the 43 peptides evaluated in vivo using microPET. Each peptide was N-terminally radiolabeled with [^{18}F]FBA and evaluated in 2 animals per timepoint. Four dynamic images were acquired and binned in 15-min increments (15, 30, 45, and 60 min postinjection), with a final single-frame 15 min image acquired ~180 min postinjection. Images shown are maximum intensity projections (MIPs) normalized to standard uptake of tracer. Data from 2 animals at the 180-min timepoint were unable to be acquired (NA). The color map is given as a function of the standard uptake estimated for each image element.

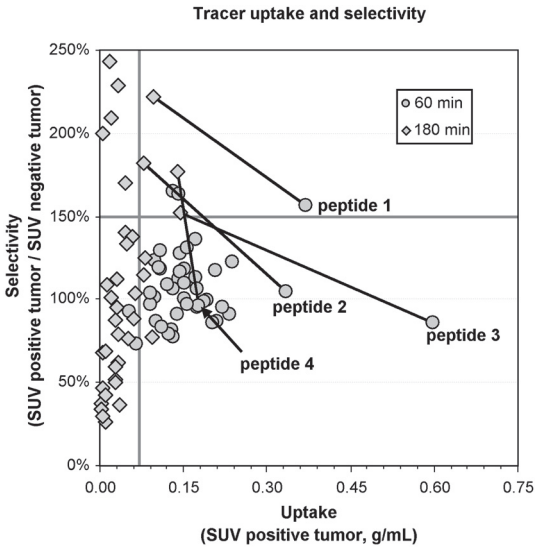

Fig. 2. Tracer properties. Scatter plot of tracer uptake (max SUV of tracer in positive tumor) and selectivity (ratio of max SUV in positive to max SUV in negative tumors) at 60 min and 180 min postinjection of [^{18}F]FBA-labeled peptide. For uptake less than 0.07 (vertical gray line), estimates were unreliable, and selectivities below 150% (horizontal gray line) were considered nonspecific.

radiochemical or mechanical, that resulted in any delays in the high-throughput imaging study.

Evaluation of the in vivo characteristics of the ^{18}F-radiolabeled peptides was conducted after reconstruction of the 3D images. The data obtained from each of the paired animal scans was reconstructed at each timepoint. Subvolumes were extracted around each animal, and the data were converted to a standard uptake value (SUV) by decay correction and normalized for injected dose and animal weight (33). These subvolumes were used for the subsequent uptake and selectivity analysis. For display purposes, maximum intensity projections (MIPs) were computed from the normalized subvolumes as shown in Fig. 1.

An ideal tumor imaging agent would have significant uptake in the positive, target-expressing tumor while having very little to no uptake in the $\alpha_v\beta_6$-negative tumor or surrounding tissues. Plotting selectivity (max SUV in the positive tumor/max SUV in the negative tumor) versus uptake (max SUV in the positive tumor; Fig. 2) revealed that after 60 min, 3 potential peptides were observed as having a high uptake in the desired target: peptide 1 ([^{18}F]FBA-RSDLTPLF), peptide 2 ([^{18}F]FBA-PGDLAVLA), and peptide 3 ([^{18}F]FBA-RTDLKKLL). Consistent with the 60-min scan, these 3 peptides also had high uptake in the desired target at the 180-min scan. These 3 peptides also displayed a good and increasing selectivity for the target at the 180-min timepoint. In addition, peptide 4 ([^{18}F]FBA-KLDLHTLE), which displayed mediocre uptake and selectivity at 60 min, showed an increase in selectivity at 180 min.

The images obtained for peptides 1–4 identified from the high-throughput in vivo study are shown in Fig. 3*A*. Significantly, these 4 peptides would not have been singled out as lead peptides solely based on the in vitro studies. [^{18}F]FBA-RSDLTPLF (peptide 1) had an IC_{50} of 15 nM for the $\alpha_v\beta_6$ integrin; this peptide also displayed potential binding to the $\alpha_{IIb}\beta_3$ and $\alpha_5\beta_1$ integrins at concentrations greater than 100 μM and no binding to the $\alpha_v\beta_3$ and $\alpha_v\beta_5$ integrins. This peptide was ranked 18th in terms of selectivity and 11th in terms of affinity. [^{18}F]FBA-PGDLAVLA (peptide 2) had an IC_{50} of 1 μM for the $\alpha_v\beta_6$ integrin; this peptide also displayed potential binding to the $\alpha_5\beta_1$ integrin at concentrations greater than 100 μM and no binding to the $\alpha_{IIb}\beta_3$, $\alpha_v\beta_3$, and $\alpha_v\beta_5$ integrins. This peptide was ranked 11th in terms of selectivity and 37th in terms of affinity. [^{18}F]FBA-RTDLKKLL (peptide 3) had an IC_{50} of 5.5 nM for the $\alpha_v\beta_6$ integrin; this peptide also displayed potential binding to the $\alpha_{IIb}\beta_3$ and $\alpha_5\beta_1$ integrins at concentrations greater than 100 μM and no binding to the $\alpha_v\beta_3$ and $\alpha_v\beta_5$ integrins. This peptide was ranked 15th in terms of selectivity and 5th in terms of affinity. [^{18}F]FBA-KLDLHTLE (peptide 4) had an IC_{50} of 15 μM for the $\alpha_v\beta_6$ integrin, binding at concentrations greater than 100 μM to the $\alpha_{IIb}\beta_3$, $\alpha_v\beta_5$, and $\alpha_5\beta_1$ integrins, and no binding to the $\alpha_v\beta_3$ integrin. Though this peptide did not meet the criteria for selectivity, it was ranked 42nd in terms of affinity. These findings are summarized in Table 2. These 4 peptides range from highly ranked, in terms of selectivity and/or affinity, to poorly ranked, based on the in vitro analysis, yet these are the peptides that performed well in vivo. In addition, we found many examples where the injected peptide displayed non-specific binding or did not bind to the target of interest. One example of a peptide that displayed non-specific binding (Fig. 3*B*) is [^{18}F]FBA-rGDLIPLL. This peptide had an IC_{50} for the $\alpha_v\beta_6$ integrin of 5 nM and was ranked 4th in terms of affinity; however, it did not meet the criteria for selectivity. One example of a peptide that was non-binding (Fig. 3*C*) is [^{18}F]FBA-RWDLH-SLR. This peptide had an IC_{50} of 33 nM for the $\alpha_v\beta_6$ integrin and, although it did not meet the criteria for selectivity, it was ranked 14th in terms of affinity. The obvious disconnect between the in vitro and in vivo results provide further evidence for the necessity of early in vivo screening.

Discussion

The aim of this work was to develop and implement a high-throughput screening approach combining peptide identification, radiolabeling with the radioactive isotope fluorine-18, and assessment of the peptides for in vivo efficacy. This approach combines the ability of OBOC chemistry to rapidly produce large peptide libraries on the solid phase, a quick, reliable, and robust solid-phase radiolabeling methodology, and in vivo evaluation using microPET imaging. This approach could allow researchers to determine early on in their investigations whether a compound is of interest before investing significant time and resources. Though we have chosen to focus on the cell-surface receptor integrin $\alpha_v\beta_6$ as the molecular target of interest, this approach is easily adaptable to any cell surface receptor or biological target.

The most common approach to developing a molecular imaging agent is through rational design, wherein the ligand/target interaction has been characterized to some degree, providing a logical starting point for the design and development of a molecular imaging agent. This is the case for cyclic RGD-based imaging agents, as well as A20FMDV2. The interest in cyclic pentapeptide RGD-based molecular imaging agents, such as RGDyK, for the $\alpha_v\beta_3$ integrin stemmed from early reports outlining RGD as the cell adhesion site in a number of proteins, such as fibronectin (34). Subsequent optimization over the past 2 decades led to the development and use of [^{18}F]galacto-RGD as the first radiotracer to successfully image $\alpha_v\beta_3$ expression in humans in 2005 (35). Similarly, the peptide that was used as our gold standard was also developed based on known ligand/binding interactions. Here, the 20-aa peptide A20FMDV2 was derived from the known sequence of the foot-and-mouth disease virus that had been shown to bind to the $\alpha_v\beta_6$ integrin (26). In vivo optimization of this peptide for use in PET is ongoing, with the addition of [^{18}F]FBA and chelates for imaging with copper-64 (36) as well as continued investigation into the optimal chemical structure for in vivo imaging (37). In both cases, initial identification of a lead sequence has led to the development of a number of related compounds, all of which have been evaluated in vivo over the course of years, to decades. By developing a high-throughput approach for the in vivo analysis of promising peptides, the potential to rapidly screen and identify the best molecular imaging agent or agents from a large number of

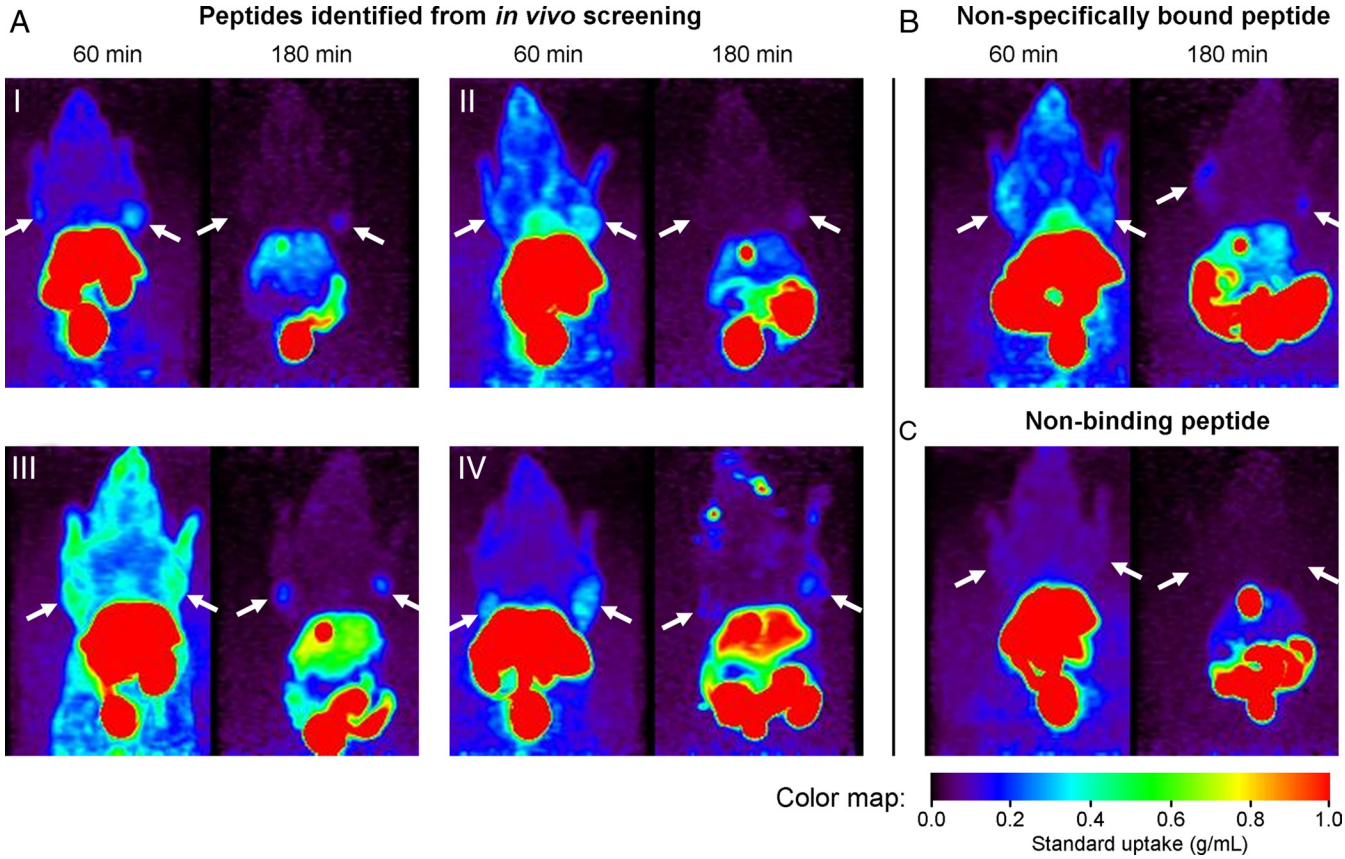

Fig. 3. MicroPET images obtained from screened peptides. The images obtained for the 4 most promising lead peptides identified from in vivo analysis are shown in *A* (I: [^{18}F]FBA-RSDLTPLF, peptide 1; II: [^{18}F]FBA-PGDLAVLA, peptide 2; III:[^{18}F]FBA-RTDLKKLL, peptide 3; IV: [^{18}F]FBA-KLDLHTLE, peptide 4). Arrows indicate location of positive and negative tumors. The animals are oriented supine and the $\alpha_v\beta_6$-positive tumor is on the right side of the mouse. All 4 of the selected animals had adequate affinity and reasonable selectivity for the positive tumor in the 180-min scan. An example of a non-specifically bound peptide ([^{18}F]FBA-rGDLIPLL) is shown in (*B*); non-specifically bound peptides had persistent uptake in both tumors. An example of a non-binding peptide ([^{18}F]FBA-RWDLHSLR) is shown in (*C*); non-binding peptides showed no uptake in either tumor.

candidates is a reality. This approach negates the dependence on lead compounds derived from known ligand/target interactions, because a wide variety of compounds can be evaluated quickly based on their in vivo binding characteristics. In addition, a family of optimized compounds could be screened, significantly reducing the time between initial discovery and clinical application.

This study presents a new approach for the identification of promising lead compounds using a high-throughput strategy. As such, we were able to screen 42 promising peptides that had been identified from the in vitro screening of several peptide libraries containing millions of compounds prepared using combinatorial chemistry. In our case, the 4 most promising peptides identified from the in vivo screen would not have been identified based solely on in vitro analysis, clearly showing the need for early in vivo analysis to identify those that may lead to viable imaging agents. The 4 peptides identified from the in vivo study had IC_{50}s that ranged from 5.5 nM (peptide 3) to 15 μM (peptide 4). Though all of the peptides contained the built-in DLX^5X^6L motif, there were no other obvious motifs that link these 4 peptide sequences. A positively charged amino acid was seen in position X^1 in peptides 1, 3, and 4. A non-polar amino acid appeared in positions X^6 and X^8 5 of 8 times (in peptides 1, 2, and 3). However, these similarities are not predictive of in vivo behavior, since other peptides that were identified from the library also contained these patterns and did not perform well in vivo.

Clearly, the in vitro analysis of large compound libraries is important and will undoubtedly remain an integral part in the identification of new molecular imaging agents. Though these in vitro screens significantly reduce the number of compounds of interest, they do not necessarily identify the best compound in terms of in vivo performance. We believe our approach has the potential to minimize the need for extensive and time-consuming in vitro analysis; by focusing our efforts on in vivo HTS using microPET, we are able to more accurately and rapidly identify the best potential targeted molecular imaging agents. Typical imaging studies investigate only one molecular imaging agent at a time; generally, only one compound is radiolabeled per day and injected into a number of animals for in vivo analysis. If that particular compound or peptide were to fail in vivo, a separate imaging study would be

Table 2. Top peptide sequences identified from in vivo analysis

Peptide	Sequence	IC_{50}	Selectivity ranking, out of 25	Affinity ranking, out of 43
1	FBA-RSDLTPLF	15	18	11
2	FBA-PGDLAVLA	1 μM	11	37
3	FBA-RTDLKKLL	5.5	15	5
4	FBA-KLDLHTLE	15 μM	n/a	42

The top 4 peptides identified from the in vivo study are shown. These peptides were chosen based on their favorable in vivo characteristics. Their IC_{50}s for the integrin $\alpha_v\beta_6$ (in nM, unless otherwise noted) are also shown along with their rankings on the selectivity/affinity lists. A total of 25 peptides were ranked with significant selectivity for the target, and 43 peptides were identified has having significant affinity. Peptide 4 did not meet the selection criteria for highly selective peptides and, therefore, did not appear on that list.

scheduled. With this study we have streamlined this process and allowed for many compounds to undergo initial in vivo screening. The in vivo study lasted a total of 11 days, and in that time we were we able to obtain over 400 images of 43 different compounds. Although thorough manual data/image analysis was required, advancements in computer technology may allow for the development of an automated screening tool to identify potential images of interest from large image arrays such as the one presented here. To the best of our knowledge, this is the first report wherein a large number of compounds have been imaged in such a short period. The high-throughput platform could be developed in such a way that allows for more than 2 animals to be evaluated per scan or different compounds may be evaluated in multiple animals per scan.

In conclusion, this report combines the benefits of OBOC chemistry, reliable solid-phase radiolabeling, and in vivo imaging using microPET to develop a high-throughput approach to identify new molecular imaging agents. This work sets the stage for the development of a high-throughput platform approach whereby a decision regarding the potential of a compound can be made rapidly using early in vivo screening. We propose to further streamline this initial high-throughput investigation through development of platform technologies for even more rapid radiolabeling, as well as increasing the number of animals that can be scanned at each timepoint. Results obtained from the in vivo HTS study will play an important role in the design and preparation of a second-generation molecular imaging library to target the $\alpha_v\beta_6$ integrin.

Materials and Methods

Library Synthesis. Peptide libraries were manually synthesized on insoluble polystyrene beads (TentaGel S NH_2; RAPP Polymere GmbH) extending from the C-terminus to the N-terminus using the OBOC combinatorial chemistry method (1, 2) and standard fluorenylmethoxycarbonyl (Fmoc) chemistry. Complete experimental details are described in *SI Text*.

Lead Compound Identification. Cell lines DX3puroβ_6 and DX3puro were used to identify positive beads from the prepared peptide libraries in cell-growth-on-bead assays (32). Experimental details are described in the text and *SI Text*.

Peptide Synthesis. Peptides were prepared manually on Rink amide resin following standard Fmoc chemistry to give the C-terminal amides. Complete experimental details are described in *SI Text*.

Competitive Binding ELISA. ELISAs were performed in triplicate at 7 concentrations on peptides N-terminally modified with FBA. Complete experimental details are described in *SI Text*.

Radiosynthesis. The automated synthesis of no-carrier added (NCA) [^{18}F]FBA was performed using a Siemens/CTI chemistry process control unit (CPCU; Siemens Medical Solutions USA) (38) and subsequently used for N-terminal solid-phase peptide radiolabeling (25). Complete experimental details are described in *SI Text*.

In Vivo Studies and MicroPET Imaging. Animal care and treatment followed protocols approved by the Animal Care and Use Committee of the University of California, Davis. All animals were imaged using a dedicated small-animal PET scanner (Focus120; Siemens Medical Solutions USA). Approximately 100–200 μCi (median: 162 μCi; range: 47–191 μCi) of the radiolabeled compound of interest was simultaneously injected intravenously into 2 animals. The dynamic scan commenced 10 min (median: 9.5 min; range: 6–27 min) after injection with 4 dynamic images acquired and binned in 15-min intervals, with a final 15 min-static image acquired at 180 min. Complete experimental details are located in the text, figure legends, and *SI Text*.

ACKNOWLEDGMENTS. The authors thank cyclotron facilities manager D. L. Kukis and the staff of the Center for Molecular and Genomic Imaging (CMGI) at the University of California, Davis, for their technical support. Gratitude is also extended to L. A. Fix (for library synthesis) and C. E. Stanecki (for ELISA development and analysis). This research was funded in part by a grant from the National Institutes of Health (CA107792 and U24 CA110804).

1. Lam KS, Lebl M, Krchnak V (1997) The ''one-bead-one-compound'' combinatorial library method. *Chem Rev* 97:411–448.
2. Geysen HM, Schoenen F, Wagner D, Wagner R (2003) Combinatorial compound libraries for drug discovery: An ongoing challenge. *Nat Rev Drug Discov* 2:222–230.
3. Szardenings M (2003) Phage display of random peptide libraries: Applications, limits, and potential. *J Recept Sig Transd* 23:307–349.
4. Uttamchandani M, Wang J, Yao SQ (2006) Protein and small molecule microarrays: Powerful tools for high-throughput proteomics. *Mol BioSyst* 2:58–68.
5. Melnick JS, et al. (2006) An efficient rapid system for profiling the cellular activities of molecular libraries. *Proc Natl Acad Sci USA* 103:3153–3158.
6. Inglese J, et al. (2006) Quantitative high-throughput screening: A titration-based approach that efficiently identifies biological activities in large chemical libraries. *Proc Natl Acad Sci USA* 103:11473–11478.
7. Nicholson RL, Welch M, Ladlow M, Spring DR (2007) Small-molecule screening: Advances in microarraying and cell-imaging technologies. *Chem Biol* 2:24–30.
8. Gomez-Hens A, Aguilar-Caballos MP (2007) Modern analytical approaches to high-throughput drug discovery. *Trends Anal Chem* 26:171–182.
9. Dittrich PS, Manz A (2006) Lab-on-a-chip: Microfluidics in drug discovery. *Nat Rev Drug Discov* 5:210–218.
10. Edwards BS, Kuckuck FW, Prossnitz ER, Ransom JT, Sklar LA (2001) HTPS flow cytometry: A novel platform for automated high throughput drug discovery and characterization. *J Biomol Screen* 6:83–90.
11. Edwards BS, Oprea T, Prossnitz ER, Sklar LA (2004) Flow cytometry for high-throughput, high-content screening. *Curr Opin Chem Biol* 8:392–398.
12. Hogemann D, Ntziachristos V, Josephson L, Weissleder R (2002) High throughput magnetic resonance imaging for evaluating targeted nanoparticle probes. *Bioconjugate Chem* 13:116–121.
13. Bock NA, Konyer NB, Henkelman RM (2003) Multiple-mouse MRI. *Magn Reson Med* 49:158–167.
14. Dazai J, et al. (2004) Multiple mouse biological loading and monitoring system for MRI. *Magn Reson Med* 52:709–715.
15. Bock NA, Nieman BJ, Bishop JB, Henkelman RM (2005) In vivo multiple-mouse MRI at 7 tesla. *Magn Reson Med* 54:1311–1316.
16. McConville P, Moody JB, Moffat BA (2005) High-throughput magnetic resonance imaging in mice for phenotyping and therapeutic evaluation. *Curr Opin Chem Biol* 9:413–420.
17. Melgar S, Gillberg P-G, Hockings PD, Olsson LE (2007) High-throughput magnetic resonance imaging in murine colonic inflammation. *Biochem Bioph Res Co* 355:1102–1107.
18. Ramirez MS, Bankson JA (2007) A practical method for 2D multiple-animal MRI. *J Magn Reson Imaging* 26:1162–1166.
19. Ramirez MS, Ragan DK, Kundra V, Bankson JA (2007) Feasibility of multiple-mouse dynamic contrast-enhanced MRI. *Magn Reson Med* 58:610–615.
20. Esparza-Coss E, Ramirez MS, Bankson JA (2008) Wireless self-gated multiple-mouse cardiac cine MRI. *Magn Reson Med* 59:1203–1206.
21. Hofmann M, Weitzel T, Krause T (2006) Ga-68-DOTATOC: Feasibility of high throughput screening by small animal PET using a clinical high-resolution PET/CT scanner. *Nucl Instrum Meth A* 569:522–524.
22. Aina OH, et al. (2007) From combinatorial chemistry to cancer-targeting peptides. *Mol Pharm* 4:631–651.
23. Peng L, et al. (2006) Combinatorial chemistry identifies high-affinity peptidomimetics against $\alpha4\beta1$ integrin for in vivo tumor imaging. *Nat Chem Biol* 2:381–389.
24. Aina OH, Sroka TC, Chen ML, Lam KS (2002) Therapeutic cancer targeting peptides. *Biopolymers* 66:184–199.
25. Sutcliffe-Goulden JL, et al. (2002) Rapid solid phase synthesis and biodistribution of 18F-labeled linear peptides. *Eur J Nucl Med Mol Imaging* 29:754–759.
26. Hausner SH, DiCara D, Marik J, Marshall JF, Sutcliffe JL (2007) Use of a peptide derived from foot-and-mouth disease virus for the noninvasive imaging of human cancer: Generation and evaluation of 4-[^{18}F]fluorobenzoyl A20FMDV2 for in vivo imaging of integrin $\alpha v\beta6$ expression with positron emission tomography. *Cancer Res* 67:7833–7840.
27. Elayadi AN, et al. (2007) A peptide selected by biopanning identifies the integrin $\alpha_v\beta_6$ as a prognostic biomarker for non-small cell lung cancer. *Cancer Res* 67:5889–5895.
28. Bates RC, et al. (2005) Transcriptional activation of integrin $\beta6$ during the epithelial-mesenchymal transition defines a novel prognostic indicator of aggressive colon carcinoma. *J Clin Invest* 115:339–347.
29. Hazelbag S, et al. (2007) Overexpression of the $\alpha_v\beta_6$ integrin in cervical squamous cell carcinoma is a prognostic factor for decreased survival. *J Pathol* 212:316–324.
30. Zhang ZY, et al. (2008) Integrin $\alpha_v\beta_6$ acts as a prognostic indicator in gastric carcinoma. *Clin Oncol* 20:61–66.
31. Kraft S, et al. (1999) Definition of an unexpected ligand recognition motif for $\alpha v\beta6$ integrin. *J Biol Chem* 274:1979–1985.
32. Lau DH, et al. (2002) Identifying peptide ligands for cell surface receptors using cell-growth-on-bead assay and one-bead-one-compound combinatorial library. *Biotechnol Lett* 24:497–500.
33. Zasadny KR, Wahl RL (1993) Standardized uptake values of normal tissues at PET with 2-[fluorine-18]-fluoro-2-deoxy-D-glucose: Variations with body weight and a method for correction. *Radiology* 189:847–850.
34. Pierschbacher MD, Ruoslahti E (1984) Cell attachment activity of fibronectin can be duplicated by small synthetic fragments of the molecule. *Nature* 309:30–33.
35. Haubner R, et al. (2005) Noninvasive visualization of the activated $\alpha_v\beta_3$ integrin in cancer patients by positron emission tomography and [^{18}F]galacto-RGD. *PLoS Med* 2:0244–0252.
36. Hausner SH, et al. (2009) Evaluation of [^{64}Cu]Cu-DOTA and [^{64}Cu]Cu-CB-TE2A chelates for targeted positron emission tomography with an $\alpha_v\beta_6$-specific peptide. *Mol Imaging* 8:111–121.
37. Hausner SH, et al. (2009) Targeted in vivo imaging of integrin $\alpha_v\beta_6$ with and improved radiotracer and its relevance in a pancreatic tumor model. *Cancer Res* 69:5843–5850.
38. Marik J, Sutcliffe JL (2007) Fully automated preparation of n.c.a. 4-[^{18}F]fluorobenzoic acid and N-succinimidyl 4-[^{18}F]fluorobenzoate using a Siemens/CTI chemistry process control unit (CPCU). *Appl Radiat Isot* 65:199–203.